



# Low Temperature Characteristics of the Metal–Superconductor NIS Tunneling Thermometer

Bayan Karimi<sup>1,2</sup> · Yu-Cheng Chang<sup>1</sup> · Jukka P. Pekola<sup>1</sup>

Received: 3 February 2022 / Accepted: 3 March 2022 / Published online: 5 April 2022  
© The Author(s) 2022

## Abstract

We discuss the temperature dependence of a common low temperature local thermometer, a tunnel junction between a superconductor and a normal metal (NIS junction). Towards the lowest temperatures its characteristics tend to saturate, which is usually attributed to selfheating effects. In this technical note, we reanalyze this saturation and show that the temperature independent subgap current of the junction alone explains in some cases the low temperature behavior quantitatively.

**Keywords** Local thermometry · NIS junction · Dynes parameter · Low-T saturation

## 1 Introduction

Tunnel junctions provide local thermometry on a chip in mesoscopic physics experiments [1–5]. A common example is the junction between a normal metal (N) and superconductor (S) with an insulating barrier (I) in between, the so-called NIS-junction. The favourable features of this sensor are as follows: (i) It probes the temperature, more precisely the energy distribution of electrons, in the normal metal, but is almost fully insensitive to the temperature of the superconductor. This way it is a truly local probe. (ii) When operated in a simple dc configuration with constant current bias, it yields a voltage output that depends practically linearly on temperature over a wide range, this way providing a simple calibration. Yet, the researchers are often puzzled about the strong deviation from such linear dependence towards the lowest temperatures. This departure from the expected behavior is often attributed to selfheating effects due to finite biasing voltage of the junction, although in reality the N electrode is, on the contrary, self-cooled

---

✉ Bayan Karimi  
bayan.karimi@aalto.fi

<sup>1</sup> Pico Group, QTF Centre of Excellence, Department of Applied Physics, Aalto University School of Science, P.O. Box 13500, 00076 Aalto, Finland

<sup>2</sup> QTF Centre of Excellence, Department of Physics, Faculty of Science, University of Helsinki, 00014 Helsinki, Finland

under these bias conditions [1]. Another obvious origin of this deviation, the subgap leakage of the junction arising from various physical mechanisms is often overlooked in this context. In this technical note we find, based on experimental data and known tunneling formulae, that this temperature-independent subgap contribution, when sufficiently large, accounts alone for the observed nonlinear dependence quantitatively.

## 2 Tunneling Current of a NIS Junction Including Subgap Leakage

We start by reviewing some central results on tunneling in a NIS junction. The golden rule based charge current in a tunneling process reads

$$I = \frac{1}{eR_T} \int d\epsilon n_S(\epsilon)[f_N(\epsilon - eV) - f_S(\epsilon)]. \quad (1)$$

Here  $f_i(x) = 1/(1 + e^{\beta_i x})$  denotes the Fermi distribution function for lead  $i = N, S$  with inverse temperature  $\beta_i = (k_B T_i)^{-1}$ ,  $n_S(\epsilon)$  is the normalized density of states of the superconductor, and  $R_T$  determines the resistance of the tunnel junction. For an ideal junction, we use the normalized density of states of Bardeen–Cooper–Schrieffer (BCS) superconductor [6], given by  $n_S^{\text{BCS}}(\epsilon) = |\epsilon| / \sqrt{\epsilon^2 - \Delta^2}$ , where  $\Delta$  is the gap of the superconductor. Due to electron–hole symmetry,  $I(-V) = -I(V)$ , we obtain a symmetric form for the charge current as

$$I = \frac{1}{2eR_T} \int d\epsilon n_S(\epsilon)[f_N(\epsilon - eV) - f_N(\epsilon + eV)]. \quad (2)$$

This equation has an important message: the  $I$ – $V$  curve depends on the distribution, i.e. temperature in N, but not at all on that in the superconductor as long as  $n_S(\epsilon)$  is temperature independent, i.e. for  $T_S \ll T_C$ , where  $T_C$  is the critical temperature of the superconductor ( $T_C \sim 1.4\text{K}$  for aluminum film). At  $T_N = 0$ , the current reads  $I = \frac{1}{R_T} \sqrt{V^2 - (\Delta/e)^2}$ , which means that in the subgap regime,  $|eV| < \Delta$ , there is no charge current,  $I = 0$ , and far above the gap  $|eV| \gg \Delta$ , we have ohmic dependence  $I = V/R_T$ . For  $\frac{\epsilon}{\Delta} \gtrsim 1$ , using the approximation for BCS DOS,  $\epsilon / \sqrt{\epsilon^2 - \Delta^2} \simeq (\sqrt{2} \sqrt{\epsilon - \Delta})^{-1}$ , where  $\epsilon = E_F$  with Fermi energy  $E_F$ , one can solve Eq. (2) analytically and we have

$$I \simeq I_0 e^{-(\Delta - eV)/k_B T_N}, \quad (3)$$

where  $I_0 = \sqrt{2\pi\Delta k_B T_N} / (2eR_T)$  [1, 3]. Equation (3) demonstrates that such a temperature dependence is universal in view of the fact that  $d \ln(I/I_0) / dV = e / (k_B T_N)$ , [2] therefore making NIS a primary thermometer in principle. Note that this is true only for an ideal junction, i.e. for BCS superconductor with DOS,  $n_S^{\text{BCS}}(\epsilon)$ . Experimentally, it is hard to have such an ideal junction. Due to subgap states, external radiation, and higher order tunneling the DOS for the junction is effectively smeared beyond that of ideal BCS typically into the form of Dynes density of states

$$n_S(\epsilon) = \left| \Re e \frac{\epsilon + i\gamma}{\sqrt{(\epsilon + i\gamma)^2 - 1}} \right|, \tag{4}$$

where  $\gamma$  is known as the Dynes parameter [7, 8]. This expression modifies the  $I$ – $V$  characteristic of the NIS junction. In the range  $eV < \Delta$ , we can use the Taylor expansion in Eq. (4) for small  $\gamma$ , and we then have  $(\epsilon + i\gamma)/\sqrt{(\epsilon + i\gamma)^2 - 1} \simeq \epsilon/\sqrt{\epsilon^2 - 1} + i\gamma/(\epsilon^2 - 1)^{3/2}$ . Substituting this expansion for DOS in Eq. (2), we have two additive terms: the first one which leads to the same result as for an ideal junction at low  $T$  given in Eq. (3) and the second term which is the low temperature leakage current of a NIS junction, given by  $I_{\text{leak}} = \frac{\Delta}{2eR_T} \int_{-eV/\Delta}^{eV/\Delta} d\epsilon \frac{\gamma}{(1-\epsilon^2)^{3/2}}$ . Here for the correction term we use  $f(\epsilon) \simeq 1 - \theta(\epsilon)$  with  $\theta(\epsilon)$  the Heaviside step function. This form is applicable for the corrections at low  $T \ll \Delta/k_B$ . The tunneling current is then given by [2]

$$I \simeq I_0 e^{-(\Delta - eV)/k_B T_N} + \frac{\gamma V}{R_T \sqrt{1 - (eV/\Delta)^2}}. \tag{5}$$

### 3 Experimental Verification of the Model

A scanning electron micrograph (SEM) of the measured thermometer is shown on the left in Fig. 1. Here we have two back-to-back NIS junctions connected in series, where superconductor (aluminum) leads are presented in blue and normal metal one (copper) in red. The  $I$ – $V$  characteristic of this SINIS structure is measured as presented

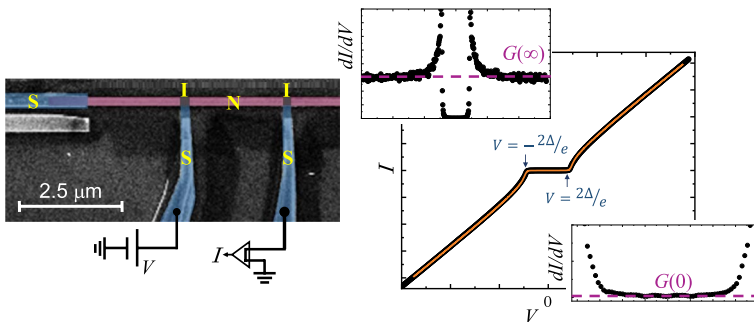


**Fig. 1** A typical SINIS structure (two NIS junctions in series). (Left panel) The SEM of SINIS with a scheme of the experimental setup. Here Cu is used as a normal metal (N), Al as a superconductor (S) and  $\text{AlO}_x$  as an insulating barrier (I). By applying a voltage bias  $V$  to the junctions, the current  $I$  through them can be measured. (Right panel) The  $I$ – $V$  characteristic of the SINIS presented shown on the left with black symbols measured at cryostat temperature  $T = 50$  mK. The resistance of the two junctions in series,  $R_T = 34$  k $\Omega$ , and superconducting gap,  $\Delta/e = 230$   $\mu\text{V}$ , can be extracted from the data, with the help of the theory fit from Eq. (2) indicated by the red line. (Insets) The conductance  $G = dI/dV$  demonstrating how to estimate the leakage parameter  $\gamma = G(0)/G(\infty)$  from the experimental data. For this sample we then obtain  $\gamma \simeq 1.6 \times 10^{-3}$  (Colour figure online)

on the right in Fig. 1. Based on the measured  $I-V$ , one can extract the value of the Dynes parameter  $\gamma$  directly. In this case,  $\gamma$  is the ratio of the zero-bias conductance of the junction  $G(0)$  to the conductance at voltages  $|eV| \gg \Delta$ ,  $\gamma = G(0)/G(\infty)$ . This principle is shown in the two insets of Fig. 1. The conductance of the junctions can be measured either directly from the  $I-V$  curve or using the derivative of it. In this figure we used the latter option. In general, one can extract three parameters for the SINIS structure (two NIS junctions in series) from the  $I-V$  characteristic presented in Fig. 1:  $\gamma$ ,  $\Delta/e$ , and  $R_T$ . For junctions that are influenced by weak superconducting proximity effect, one predicts that the Dynes parameter  $\gamma$  obeys the relation  $\gamma \sim R_K/(nR_T)$  where  $R_K = h/e^2 \simeq 25.8 \text{ k}\Omega$ , the von Klitzing constant, denotes the resistance quantum and  $n$  refers to the effective number of conduction channels in the junction,  $n = A/A_{\text{ch}}$  [9]. Here  $A_{\text{ch}}$  stands for the effective area of one conduction channel. According to previous experiments  $A_{\text{ch}} \sim 30 \text{ nm}^2$ , and the junction area  $A \sim 150 \times 150 \text{ nm}^2$  which is estimated roughly from the scanning electron micrograph. We have then  $\gamma \sim 1 \times 10^{-3}$  which is of the same order of magnitude as from our experimental estimate,  $\gamma = 1.6 \times 10^{-3}$ . In junctions not affected by Andreev effects, the microwave radiation yields the dominant contribution of  $\gamma$  [10]. Next, we use the parameters  $\gamma$ ,  $R_T$ , and  $\Delta/e$  and simulate the  $I-V$  curves at various temperatures based on Eq. (2) with the help of Eq. (4) for describing the DOS of the actual sample. This set of curves is presented in Fig. 2a. It is clear that by increasing temperature, the  $I-V$  curves become increasingly smeared. The zoom-out of this panel shows the  $I-V$ s in a narrow current range. Basic temperature measurement is done by applying a fixed current  $I_m$  to the SINIS (or NIS) structure. This way the voltage across the junction is changing as a function of temperature and thus this measurement works as a calibration for our system. Figure 2b displays such calibrations for different values of  $\gamma$ . The leakage  $\gamma$  plays an important role in determining the sensitivity of the thermometer. It is vivid that for small  $\gamma$ s the thermometer is sensitive down to low temperatures while by increasing it the curves saturate at low  $T$  at the voltage  $V_0$  given by

$$V_0 = \frac{I_m R_T}{\sqrt{\gamma^2 + \left(\frac{eI_m R_T}{\Delta}\right)^2}}, \quad (6)$$

obtained by setting  $T_N = 0$  and  $I \equiv I_m$  in Eq. (5). The experimental data is shown as symbols in the same panel and matches quantitatively with the predicted dependence using the independently determined parameters  $\gamma$ ,  $R_T$  and  $\Delta/e$  (no extra fit parameters).

Responsivity  $\mathcal{R}$  is an important figure of merit of a sensor which is defined as the change of the measured quantity (here voltage) with respect to temperature, meaning  $\mathcal{R} = dV/dT$ . Using Eq. (5), one can compare  $\mathcal{R}$  of the SINIS thermometer in the presence,  $\mathcal{R}(\gamma)$ , and absence,  $\mathcal{R}(\gamma = 0)$ , of the leakage as

$$\frac{\mathcal{R}(\gamma)}{\mathcal{R}(\gamma = 0)} \equiv \frac{dV/dT}{(dV/dT)_{\text{ideal}}} = \left( 1 + \gamma \frac{k_B T}{eR_T \left( I_m - \frac{\gamma V}{R_T} \right)} \right)^{-1}. \quad (7)$$

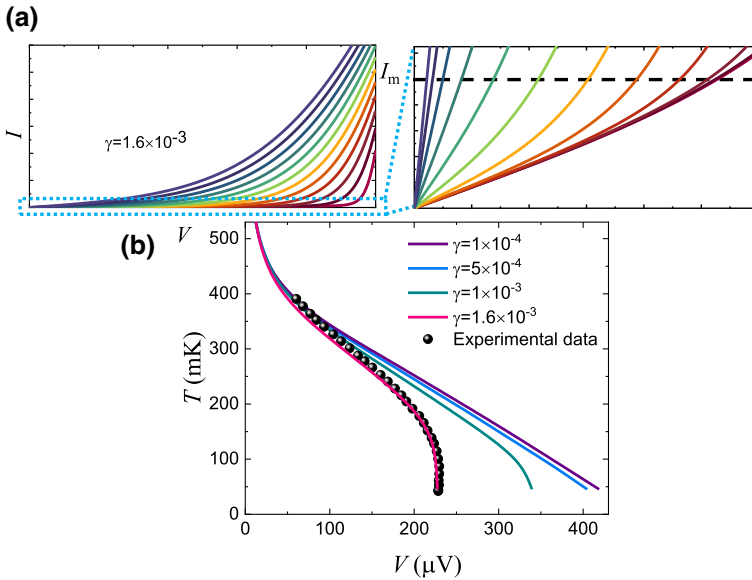


**Fig. 2** The role of leakage parameter  $\gamma$  in calibration of the thermometer. **a** Calculated  $I$ – $V$  characteristics of the SINIS structure presented in the left panel of Fig. 1 from Eq. (2) at different temperatures, with parameters  $R_T = 34 \text{ k}\Omega$  and  $\Delta/e = 230 \text{ }\mu\text{V}$ . The zoom of the light blue rectangle is presented in the inset. The presence of the leakage,  $\gamma$ , induces a slope in the subgap region which leads to sensitivity loss at low temperatures. Applying a fixed current  $I_m$  (dashed black line), one can extract voltages at different temperatures which gives a thermometer. Calibrations of such a thermometer for different values of  $\gamma$  are presented in panel **b** with a few values of  $\gamma$ . When increasing  $\gamma$  the calibration saturates at low temperature. The experimental data shown with black symbols catches the curve presenting  $\gamma = 1.6 \times 10^{-3}$ , which is obtained as in Fig. 1.  $I_m = 15 \text{ pA}$  for all the data in (b) (Colour figure online)

Equation (7) indicates that responsivity of the thermometer decreases with increasing leakage current, as one might expect.

## 4 Discussion

Although a NIS junction serves as a convenient local thermometer especially at subkelvin temperatures, it suffers from various non-idealities. Here we showed that for junctions where temperature-independent leakage is relatively strong, which is the case in many experiments, this effect fully determines the low temperature characteristics of the thermometer, and it leads to the loss of sensitivity. Yet we want to underline that it is possible to achieve much lower leakage,  $\gamma \ll 10^{-4}$ , in setups with high-quality junctions if the superconducting proximity effect and external noise are effectively suppressed; then other factors, e.g. nonequilibrium effects, may play the dominant role in determining the low-temperature transport. In this note we focused on dc measurement of the junction but similar considerations apply also for rf detection of junction conductance [11].

**Acknowledgements** We received funding from the Academy of Finland under Grant 312057. We acknowledge the provision of facilities and technical support by Aalto University at the OtaNano—Miconova Nanofabrication Center and through the low temperature laboratory (LTL) infrastructure, which is part of the EU Horizon 2020 European Microkelvin Platform (EMP), No. 824109.

**Funding** Open Access funding provided by Aalto University.

**Data Availability** Data will be made available upon reasonable request.

**Open Access** This article is licensed under a Creative Commons Attribution 4.0 International License, which permits use, sharing, adaptation, distribution and reproduction in any medium or format, as long as you give appropriate credit to the original author(s) and the source, provide a link to the Creative Commons licence, and indicate if changes were made. The images or other third party material in this article are included in the article's Creative Commons licence, unless indicated otherwise in a credit line to the material. If material is not included in the article's Creative Commons licence and your intended use is not permitted by statutory regulation or exceeds the permitted use, you will need to obtain permission directly from the copyright holder. To view a copy of this licence, visit <http://creativecommons.org/licenses/by/4.0/>.

## References

1. F. Giazotto, T.T. Heikkilä, A. Luukanen, A.M. Savin, J.P. Pekola, Opportunities for mesoscopies in thermometry and refrigeration: physics and applications. *Rev. Mod. Phys.* **78**, 217 (2006)
2. A.V. Feshchenko, L. Casparis, I.M. Khaymovich, D. Maradan, O.-P. Saira, M. Palma, M. Meschke, J.P. Pekola, D.M. Zumbühl, Tunnel-junction thermometry down to millikelvin temperatures. *Phys. Rev. Appl.* **4**, 034001 (2015)
3. M. Nahum, J.M. Martinis, Ultrasensitive-hot-electron microbolometer. *Appl. Phys. Lett.* **63**, 3075 (1993)
4. J.P. Pekola, B. Karimi, Colloquium: quantum heat transport in condensed matter systems. *Rev. Mod. Phys.* **93**, 041001 (2021)
5. H. Courtois, F.W.J. Hekking, H.Q. Nguyen, C.B. Winkelmann, Electronic coolers based on superconducting tunnel junctions: fundamentals and applications. *J. Low Temp. Phys.* **175**, 799 (2014)
6. J. Bardeen, L.N. Cooper, J.R. Schrieffer, Theory of superconductivity. *Phys. Rev.* **108**, 1175 (1957)
7. R.C. Dynes, V. Narayanamurti, J.P. Garno, Direct measurement of quasiparticle-lifetime broadening in a strong-coupled superconductor. *Phys. Rev. Lett.* **41**, 1509 (1978)
8. R.C. Dynes, J.P. Garno, G.B. Hertel, T.P. Orlando, Tunneling study of superconductivity near the metal-insulator transition. *Phys. Rev. Lett.* **53**, 2437 (1984)
9. T. Greibe, M.P.V. Stenberg, C.M. Wilson, T. Bauch, V.S. Shumeiko, P. Delsing, Are “pinholes” the cause of excess current in superconducting tunnel junctions? A study of Andreev current in highly resistive junctions. *Phys. Rev. Lett.* **106**, 097001 (2011)
10. J.P. Pekola, V.F. Maisi, S. Kafanov, N. Chekurov, A. Kemppinen, Y.A. Pashkin, O.-P. Saira, M. Mötönen, J.S. Tsai, Environment-assisted tunneling as an origin of the Dynes density of states. *Phys. Rev. Lett.* **105**, 026803 (2010)
11. B. Karimi, J.P. Pekola, Noninvasive thermometer based on the zero-bias anomaly of a superconducting junction for ultrasensitive calorimetry. *Phys. Rev. Appl.* **10**, 054048 (2018)

**Publisher's Note** Springer Nature remains neutral with regard to jurisdictional claims in published maps and institutional affiliations.